Experimental evaluation of mechanical and electrical power consumption of feed drive systems driven by a ball-screw

Rigacci, Massimiliano
Sato, Ryuta
Shirase, Keiichi

(Citation)
Precision Engineering, 64:280-287

(Issue Date)
2020-07

(Resource Type)
journal article

(Version)
Accepted Manuscript

Title

Experimental evaluation of mechanical and electrical power consumption of feed drive systems driven by a ball-screw

Author names and affiliation

Massimiliano Rigacci, Ryuta Sato, and Keiichi Shirase

Department of Mechanical Engineering, Kobe University, 1-1 Rokkodai, Nada, Kobe, 657-8501, Japan

Corresponding author

Ryuta Sato

Department of Mechanical Engineering, Kobe University, 1-1 Rokkodai, Nada, Kobe, 657-8501, Japan

Email: sato@mech.kobe-u.ac.jp

Abstract

An experimental analysis of the mechanical and electrical power consumption of feed drive systems is presented in this paper. The main components affecting the power consumption are the motor, bearings, ball-screw, and table. The power consumption of the motor has been investigated experimentally through the study of the electrical efficiency. The efficiency has been calculated from the acquired angular velocity and supplied torque for several velocities and loads. The study shows how the working conditions of the motor heavily influence the efficiency of the motor and therefore the power consumption of the whole feed drive system. Moreover, the mechanical power consumption of each component of the feed drive has been investigated, showing that the main component responsible for the consumption is the ball-screw. Thus, in order to clarify the influence of the constructive parameters of the ball-screw on the power consumption, four kinds of ball-screws differing in the lead dimension and the preload condition have been considered. Furthermore, it clarifies the relation between the power consumption of the feed drive system and the working velocity of the table. Finally, the advantages and disadvantages of each feed drive mechanical configuration are discussed, emphasizing that the driven factor that affects the power consumption the most is the angular velocity, due to the trade-off between the motor efficiency and the mechanical power loss from the friction of the components in relative motion. This research can help the selection of the lead of the ball-screw, from an energetic point of view, in order to get higher efficiency of the feed drive.

Keywords

Feed drive system, Ball-screw, Power consumption, Motor efficiency, Mechanical power consumption

1. Introduction

In the last years, the necessity to reduce the impact of human activities on the surrounding environment has led many researchers to focus their attention on the problem of energy consumption, especially in the manufacturing field. Feed drive systems occupy a special position in manufacturing because, due to their characteristics, they are widely employed in the production of semiconductors and machine tools, to cite just a few.

Many researchers [1-6] have investigated several methods to evaluate the energy consumption of machine tools. Hayashi et al. have investigated the energy consumption of feed drive systems considering both the electrical losses due to the amplifier and the mechanical losses due to the friction of the system [7]. Several studies have been conducted on the efficiency of permanent magnet synchronous motors showing how much the efficiency of the motor depends on the torque-velocity characteristic [8-18]. Other researchers investigated the efficiency of ball-screws [19-21], showing that efficiency is affected mainly by friction, angular velocity, and axial load applied to the ball-screw. However, while most of the studies focus on the energy consumption of the whole feed drive system, it is still not clear how much energy each component of the feed drive consumes.

Therefore, in this research, the power consumption of a feed drive system has been investigated experimentally for each component. The efficiency map of the motor is calculated through a novel experimental set-up, for several velocities and supplied torque, and several experiments are performed to determine the amount of mechanical power consumed by each component. Thus, the mechanical power consumption (M.P.C.) of the system, considering four kinds of ball-screws differing in the lead of the screw and the preload condition, is investigated; moreover, it is found that for many of the tested ball-screws the motor works with low efficiency. Finally, it is clarified which ball-screw ensures the lowest power consumption. This research offers, therefore, a guidance for the selection of the screw lead and it can particularly benefit mass production applications.

2. Experimental apparatus

2.1. Feed drive system

The feed drive system is composed of a servo motor, a coupling, two support bearings, a ball-screw, and two linear guides supporting the table (Fig. 1). The servo motor is a three-phase Permanent Magnet Synchronous Motor (Yaskawa Electric SGMGV-05ADA21) and its main constructive parameters are enlisted in Table 1. The ball-screw (THK) is supported by two ball bearings: the one placed toward the motor side performs the angular constraint while the one on the opposite is a deeply grooved bearing. The screw is, therefore, constrained in ISO constrained configuration. The nut of the ball-screw is joint to the table and the table slides over two parallel linear guides. Globally, four ball-screws are considered; the main constructive parameters of each ball-screw are enlisted in Table 1. In Table 1, the ball-screw lead, nut preload method, and nut rotation torque are specified. Ball-screws A, B, and C are single nut-type screws with different leads (i.e., 20, 10, and 5 mm, respectively), while Ball-screw D is a double nut-type screw with a 5 mm lead. Controlling the pre-load is difficult; hence, the rotational torque of the nut, when it starts the rotation, is measured for each screw. From Table 1, it is evident that the rotational torque of Ball-screw D is more than two times larger than that of Ball-screw C. The difference is expected to affect the power consumption. The velocity control system, Proportional-Integral (Fig. 2), is built on the angular velocity detected by the rotary encoder on the motor. The system is implemented by a computer with a DSP board (dSPACE DS1104).

2.2. Measurement method for electric power consumption

In order to measure the electric power consumption of the motor, an apparatus such as the one in Fig. 3 is used. The apparatus consists of two differential probes to measure the voltages and two amperometric clamps to measure the currents. The electric voltage is scaled 1/1000 and recorded along with the current by an AD converter in the DSP board. Moreover, the signal is amplified, and an analog low-pass filter with 1600 Hz cutoff frequency is used to avoid aliasing. The data sampling frequency is set to 4000 Hz. Since the motor is a three-phase motor without neutral wire, it is possible to calculate the electric power consumption using two of the three currents and voltages, as demonstrated by Eq. (1):

$$P = E_1 I_1 + E_2 I_2 + E_3 I_3 = W_a + W_b + W_c$$
$$I_1 + I_2 + I_3 = 0$$
$$P = E_1 I_1 + E_2(-I_1 - I_3) + E_3 I_3 \tag{1}$$
$$P = (E_1 - E_2)I_1 + (E_3 - E_2)I_3 = V_{12}I_1 + V_{32}I_3 = W_a + W_b$$

Where E_1, E_2 and E_3 are the voltages of each phase, I_1, I_2 and I_3 are the currents of each phase, W_a, W_b and W_c are the electric powers of each phase. Therefore, from the signal of current and voltage, the root mean square values are calculated, according to Eq. (2):

$$V_{rms} = \sqrt{\frac{1}{n}\sum_{k=1}^{n}\{V_k\}^2}$$
$$I_{rms} = \sqrt{\frac{1}{n}\sum_{k=1}^{n}\{I_k\}^2} \tag{2}$$

Where V_k and I_k are the *k-th* voltage and current respectively. In order to measure the electric efficiency of the motor, the apparatus shown in Fig. 4 is used; it consists of two servo motors facing each other and connected through a coupling. Motor A works as a motor and motor B as a load; both motors are controlled by the same DSP board. The mechanical power supplied by the motor is calculated from the torque and angular velocity detected by the controller. Once the signal has been acquired, the average value is calculated as in Eq. (3):

$$\tau_{ave} = \frac{1}{n}\sum_{k=1}^{n}\tau_k$$
$$\omega_{ave} = \frac{1}{n}\sum_{k=1}^{n}\omega_k$$
$$P_{mech} = \tau_{ave} * \omega_{ave} \tag{3}$$
$$P_{overall} = \sum_{k=1}^{2} V_k I_k$$
$$P_{electric} = P_{overall} - P_{mech}$$

Where τ_k and ω_k are the torque and angular velocity respectively, and $P_{overall}$, P_{mech}, and P_{elec} are the overall power, mechanical power, and electrical power, respectively. Thus, the efficiency η_e is calculated according to Eq. (4):

$$\eta_e = \frac{\tau_{ave}\omega_{ave}}{\sum_{k=1}^{2} V_k I_k} \tag{4}$$

3. Evaluation of motor efficiency

3.1. Measurement method

In order to evaluate the electric efficiency of the motor, several tests are performed. Each test consists of 24 angular velocities from 1 to 70 rad/s (from approximately 10 to 670 rev/min) imposed through a velocity control of motor A. Motor B offers a constant load torque during each test; 15 torque values from 0 to 2.7 Nm are considered. For each velocity, the rotation in both the directions are considered; thus, since a positive rotation of motor A means a clockwise motion, a positive load for motor B means an opposition toward the relative rotation (the motors are facing each other) while a negative torque means a pull toward the rotation sense of motor A. In Figs. 5 and 6, the signals of torque, angular velocity, voltage, and current in the case of load torque of 0.3 Nm provided by motor B are shown. It is evident that both torque and current that the motor supplies are higher when the load opposes the relative motion (Figs. 5 and 6, load torque in opposition) compared to the case of load torque concurrent to the torque supplied by motor A. The difference is appreciable for both the values of torque and current and the relative amplitudes of the fluctuation. For each velocity, only the case when the load opposes the rotation of motor A is considered, in order to make an actual resistive load. For each test, only the constant velocity part of the signal is considered; thus, the average values of torque and angular velocity and the rms of voltage and current are calculated according to Eq. (3). The efficiency is therefore calculated through Eq. (4), thus the mean between the clockwise and anticlockwise rotation (and the relative loads) is performed.

3.2. Evaluated efficiency

The evaluated efficiency map of the motor is shown in Fig. 7. According to the result, the efficiency of the motor significantly depends on the rotational velocity and loading torque conditions. The efficiency of the motor drops when the velocities become lower. The evaluation test is carried out up to approximately 670 rev/min because the typical moving velocity of feed drive systems in the machine tools is lower than the rated velocity of the motors, although the rated velocity of the motor is 1500 rev/min. When a constant velocity is imposed on the motor, the efficiency depends on the loading torque, and the optimum loading torque exists for each rotational velocity.

4. Power consumption of each component

One of the primary purposes of this research is the evaluation of the power consumption of each component of the feed drive system with respect to the total power input in the system. Therefore, after the analysis of the motor power consumption, the study of the M.P.C. of each component is necessary. The power consumption of the feed drive system is measured without any applied load and for several constant table velocities; thus, the power consumption is due only to the frictions from the relative motion of each component.

4.1. Measurement method

In order to investigate the relationship between the M.P.C. of the feed drive and the table working velocity, 11 velocities from 6 to 60 mm/s are imposed to the table through a positional command by adding a position control loop to the controller. The measurement tests with various velocity are carried out with a specially designed positional command. The positional command consists of 11 cycles of the reciprocated motion; the tested velocities are distributed according to ISO3:1973 (preferred number series) and are, therefore, 6, 7.5, 9.6, 12, 15, 18.9, 24, 30, 37.8, 48, and 60 mm/s. Each motion cycle includes 15 rotations of the motor; for each test condition, the signals of torque and angular velocity are acquired for one second in the central part of the constant velocity motion (Fig. 8). Thus, the average value is calculated according to Eq. (3).

4.2. Measurement condition

Four components in the feed drive system are responsible for the M.P.C.: motor, bearings, ball-screw nut, and the linear ball guides. In order to investigate the contribution of each component on the overall power consumption, the system is disassembled and each component is individually considered. First, the motor is taken alone, the position loop is imposed, and the torque and angular velocity signals are acquired in the constant velocity part (Fig. 8); the M.P.C is calculated through Eq. (5). In this way, the power consumption -velocity characteristic relation of the motor is determined. Then, the motor is considered along with the bearings; to do so, the motor is joined to the ball-screw, but the ball-screw nut is not joined to the table; therefore, there is no relative motion between ball-screw and nut. Thus, there is no power consumption due to the ball-nut friction. The power consumption for each velocity is, thus, calculated through Eq. (6). The contribution of the bearings to the power consumption is calculated through Eq. (7). In order to determine the contribution of the linear ball guides on power consumption, a linear motor is considered. The linear motor is installed on the table. The setup conditions are described in [7]. The table is then disconnected from the nut of the ball-screw; thereby, the relationship between velocity and power consumption is identified, and the power consumption due to the linear guides is calculated through Eq. (8). The effect of the linear motor weight on the friction characteristic of the linear guides, and therefore the power consumption, is considered negligible due to the weak weight-friction relationship for the linear ball guides [22]. Finally, the position is commanded to the fully assembled system (the feed drive with all its components), and the power consumption is calculated through Eq. (9). The contribution of the ball-screw nut joint on the power consumption due to friction is calculated subtracting the contribution of each previously calculated component from the full system power consumption, as presented in Eq. (10). The total M.P.C. is defined by Eq. (11) as having an identical value with Eqs. (3) and (10).

$$P_{motor} = \tau^{motor}_{ave} * \omega^{motor}_{ave} \tag{5}$$

$$P_{m+b} = \tau^{m+b}_{ave} * \omega^{m+b}_{ave} \tag{6}$$

$$P_{bearing} = P_{m+b} - P_{motor} \tag{7}$$

$$P_{LG} = F^{LG}_{ave} * v^{LG}_{ave} \tag{8}$$

$$P_{FS} = \tau^{FS}_{ave} * \omega^{FS}_{ave} \tag{9}$$

$$P_{Nut} = P_{FS} - P_{LG} - P_{m+b} \tag{10}$$

$$P_{mech} = P_{motor} + P_{bearing} + P_{LG} + P_{nut} \tag{11}$$

where P_{motor}, P_{m+b}, $P_{bearing}$, P_{LG}, P_{FS}, and P_{Nut} are the power consumptions of the motor, motor and bearing, bearing, linear guides, full system, and nut, respectively. F^{LG}_{ave} and v^{LG}_{ave} denote the force and the velocity of the linear motor, respectively.

4.3. Evaluated power consumption of each component

Figure 9 shows the evaluated power consumption of each component of the system. The power consumption can be classified to M.P.C. of each mechanical component and electric power consumption of the motor. The M.P.C. means the power consumption due to the frictions, and the electric power consumption means the loss of the motor due to its efficiency. The colored lines represent the M.P.C. of each component; the total M.P.C. is represented by the dark green arrow on the right side of the figures. The arrow length represents the amplitude of the power consumption of each component; depending on the velocity of the table, the amplitude of the power consumption of each component changes; but, for all the velocities considered, the ball-screw nut joint (purple arrow) represents the most of the M.P.C., accounting approximately for the 60% - 70% for the 60 mm/s case. Each line shows the amount of the power consumption of each component; in all the cases, the consumption increases approximately linearly with the table velocity, indicating that the viscous friction is very small. Moreover, the components that account for a majority of the power consumption are the ball-screw, the bearings, and the motor. The power consumption of bearings become higher for the ball-screw C and D because the smaller the lead, the higher is the angular velocity; thus, the friction component becomes higher. In Table 1, the rotational torque of each ball-screw nut is listed. The rotational torque must be supplied to the nut to win the static friction and put the nut in relative motion with respect to the screw. Note that the preload force is very difficult to quantify and control; therefore, only the rotational torque is considered as a preload indicator. Ball-screw D has a static rotational torque that is more than two times that of Ball-screw C. Considering Fig. 9 (c) and (d), because both the ball-screws have a lead of 5 mm, it becomes clear that increasing the preload of the ball-screw increases the M.P.C. Moreover, considering Figs. 9(b) and (c), we can compare the effects of lead for ball-screws with a similar static rotational torque, but different leads. The angular velocity of Ball-screw B at 60 mm/s is the same as the table velocity at 30 mm/s of Ball-screw C. The power consumed by the screw–nut joint of Ball-screw B for the table velocity at 60 mm/s is 5.36 W, while that for Ball-screw C is 4.45 W. The power values are close to each other. The difference in the values is expected to come from the influence of the velocity dependency of the friction torque of each component. The rotational torque is a static torque; therefore, the proportion between the lengths of the arrows of the nut power consumption in Fig. 9 is only indicative. Fig. 10 shows the comparison between the overall power consumption of the four ball-screws; the lowest power consumption is for the ball-screw A and the highest for the ball-screw D.

5. Power consumption of a feed drive system

The overall power consumption of the feed drive system depends both on the power dissipated by the friction of its components and on the power waste caused by the motor inefficiency. In Fig. 9, the light blue arrow represents the electric power consumption due to the motor "inefficiency." It represents, therefore, the amount of power that is wasted by the motor because the efficiency is lower than one; if the motor efficiency were one, the light blue arrow would coincide with the purple one. The brown arrow represents the overall power consumption of the feed drive; that is, the addition of the dark green and light blue arrows magnitude. Moreover, the ratio between the electric power consumption (light blue arrow) and the overall power consumption (brown arrow) represents the complementary to one of the efficiency (1-η_e) of the motor; the lower velocity, the higher the ratio; therefore, the lower is the most efficient.

Figures 11 and 12 show the comparisons of the power consumption between two table velocities: 12 mm/s (a) and 48 mm/s (b), selected from the 11 velocities of the previous evaluation test (see section 4.1). Fig. 11 shows the M.P.C. and Fig. 12 shows the overall power consumption of the system. In both cases, the M.P.C. necessary to keep the table velocity constant increases, decreasing the lead of the ball-screw. The table velocity is fixed; hence, for ball-screws with a smaller lead, the motor must supply a higher angular velocity. Although the friction torque is constant, it produces more power because power is represented as the product of torque and angular velocity. The 48 mm/s case shows a higher power consumption compared to the 12 mm/s case because the velocity is higher. The overall power consumption of the feed drive system, that is the total electric power entering the system, grows with the velocity and its increase decreases the lead of the ball-screw; a higher overall power is necessary to overcome the higher friction loss. The beforehand trend is common to all the velocities and ball-screw exception for the 12 mm/s case 10 mm ball-screw. The reason why that case shows an inverted trend in respect to the others is that for constant velocity motion the overall electric power consumption depends on two terms: the power necessary to overcome the friction loss and the power waste caused by the motor's low efficiency.

The operative points on the efficiency map for each ball-screw for both the 12 and 48 mm/s velocities are shown in Fig. 13. The operative points are identified based on the average torque and angular velocity calculated from the experimental data. Meanwhile, the efficiency values are predicted by the efficiency map once the average torque and angular velocity are known. Considering Fig. 12 (a), the M.P.C. in the case of 20 mm lead is slightly higher than that in the 10 mm case, while the overall electric power is lower for the lead of 10 mm (because the angular velocity is higher), the motor works in a higher efficiency zone (Fig. 13). It can be seen that the ball-screw A with 12 mm/s case works in a very low-efficiency area while ball-screw B works in a slightly higher efficiency area; thus, since the power wastage caused by friction is almost the same in both the cases, the increased efficiency reduces the overall electric power consumption for the ball-screw with a 10 mm lead. The only exception is in the case of the 10 mm lead. In all the other cases, the growth of the M.P.C. is higher than the reduction in electric power due to an increment in efficiency; therefore, the overall electric power consumption is higher. The overall electric power consumption is a trade-off between two opposite trends: the increment of the M.P.C. with an increase in velocity and the decrement of electric power consumption due to an increase in the motor efficiency as shown in Fig. 14. The motor efficiency values in Fig. 13 are slightly different from those in Fig. 14. The efficiency map is measured using the apparatus shown in Fig. 4, although the efficiency in Fig. 14 is measured considering the feed drive mechanism. The apparatus in Fig. 4 ensures the control of both the motor and load torque. However, in the experiments performed using the feed drive mechanism, the motor torque is affected by several sources, such as friction fluctuation and mechanical vibration. This result indicates that other factors affecting the motor efficiency exist. The maximum difference for Ball-screw C is approximately 22% of the value predicted in Fig. 14. We will try to clarify the influence of the vibration condition on the motor efficiency.

6. Conclusions

In this study, the power consumption of a feed drive system driven by ball-screws has been analyzed. The overall power consumption is due to the addition of the motor electric power consumption and the M.P.C. from friction. The motor efficiency has been evaluated through a novel apparatus and the M.P.C. is evaluated component by component. In general, the following conclusions can be summarized:

1) The electric power consumption of the motor and its efficiency depend strongly on the angular velocity and the supplied torque.

2) The overall power consumption of the feed drive increases with the velocity; moreover, most of the M.P.C. is due to low efficiency in the screw-nut joint and electric motor.

3) The larger lead of the ball-screw has the least M.P.C. The motor efficiency has an opposite trend.

4) When assigned a table working routine, the overall power consumption depends strongly on the lead of the selected ball-screw because the lead determines the motor angular velocity and, therefore, both the electric and mechanical power losses.

This research, therefore, clarifies both, the M.P.C. of each component of the feed drive and the relation, for the constant velocity motion, among the lead of the screw, the motor efficiency, and the power consumption. In the future work, we will expand the research on the study of the M.P.C and motor electric efficiency for the transient motion. Moreover, we will investigate the mechanical efficiency of the ball-screw in order to perform an optimization of the power consumption of feed drive systems. We will also try to clarify the reasons for the difference between the efficiency predicted in Fig. 13 and that calculated from the experiments (Fig. 14). Moreover, it is probable that the electric and mechanical efficiencies can determine the heat generated by each part. We will try to investigate and predict the amount of heat generation due to electrical losses in the motor and friction.

References:

1. Rahimifard, S., Seow, Y., Childs, T., Minimizing embodied product energy efficient manufacturing, CIRP Annals-Manufacturing Technology, 59 (2010) 25-28.
2. Neugebauer, R., Wabner, M., Rentzsch, H., Ihlenfeldt, S., Structure principles of energy efficient machine tools, CIRP J. Manuf Sci. Technol., 4, 2 (2011) 136-147.
3. Shaohua, H., Fei, L., Yan, H., Tong, H., An on-line approach for energy efficiency monitoring of machine tools, J. Cleaner Prod, 27 (2012) 133-140.
4. Mori, M., Fujishima, M., Inamasu, Y., Oda, Y., A study on energy efficiency improvement for machine tools, CIRP Ann. Manuf. Technol., 60, 1 (2011) 145-148.
5. Gotze, U., Koriath, H.J., Kolesnikov, A., Lindner, R., Paetzold, J., Integrated methodology for the evaluation of the energy, CIRP Journal of Manufacturing Technology, 5, 3 (2012) 151-163.
6. Diaz, N., Ninomiya, K., Noble, J., Dornfeld, D., Environmental impact characterization of milling and implications for potential energy savings in industry, Procedia CIRP, 1 (2012) 518-523.
7. Hayashi, A., Iwase, R., Sato, R., Shirase, K., Measurement and simulation of energy consumption of feed drive systems, Journal of Mechanics Engineering and Automation, 4 (2014) 203-212.
8. Caricchi, F., Crescimbini, F., Fedeli, E., Noia, G., Design and construction of a wheel directly-coupled axial-flux PM motor prototype for EVs, Proceedings of 1994 IEEE Industry Applications Society Annual Meeting, (1994) Denver, CO, USA.
9. Peralta-Sanchez, E., Smith, A.C., Rodriguez-Rivas, J.J., Steady-state analysis of a canned line-start PM motor, IEEE Transactions on Magnetics, 47, 10 (2011) 4080-4083.
10. Morimoto, S., Tong, Y., Takeda, Y., Hirasa, T., Loss minimization control of permanent magnet synchronous motor drives, IEEE Transactions on Industrial Electronics, 41, 5 (1994) 511-517.
11. Cavallaro, C., Oscar, D., Tommaso, A., Miceli, R., Raciti, A., Galluzzo, G.R., Trapanese, M., Efficiency enhancement of permanent-magnet synchronous motor drives by online loss minimization approaches, IEEE Transactions on Industrial Electronics, 52, 4 (2005) 1153-1160.
12. Takahashi, I., Koganezawa, T., Su, G., Ohyama, K., A super high speed PM motor drive system by a quasi-current source inverter, IEEE Transactions on Industry Applications, 30, 3 (1994) 683-690.
13. Kim, W.-H., Kim, K.-C., Kim, S.-J., Kang, D.-W., Go S.-C., Lee H.-W., A study on the optimal rotor design of LSPM considering the starting torque and efficiency, IEEE Transactions on Magnetics, 45, 3 (2009) 1808-1811.
14. Sim, D.-J., Cho, D.-H., Chun, J.-S., Jung, H.-K., Efficiency optimization of interior permanent magnet synchronous motor using genetic algorithms, IEEE Transactions on Magnetics, 33, 2 (1997) 1880-1883.
15. Patel, H.K, Nagarsheth, R, Parnerkar, S., Performance comparison of permanent magnet synchronous motor and induction motor for cooling tower application, International Journal of Emerging Technology and Advanced Engineering. 2, 8 (2012) 167-171.
16. Lei, Y., Zhang, Y., Huang, W., Accurate and efficient torque control of an interior permanent magnet synchronous motor in electric vehicles based on hall-effect sensors, Energies, 10, 3 (2017) doi: 10.3390/en10030410.
17. Kurihara, K., Rahman, M.A., High efficiency line-start interior permanent magnet synchronous motors, IEEE Transactions on Industry Applications, 40, 3 (2004) 789-796.
18. Lin, M.C., Velinsky, S.A., Ravani, B., Design of the ball screw mechanism for optimal efficiency, Trans. ASME, 116 (1994) 856-861.
19. Wei, C.C., Lin, J.F., Kinematic analysis of the ball screw mechanism considering variable contact angles and elastic deformations, Journal of Mechanical Design, 125 (2003) 717-733.
20. Wei, C.C., Lin, J.F., Analysis of a ball screw with a preload and lubrication, Tribology International, 42 (2009) 1816-1831.
21. Wei, C.C., Lin, J.F., Kinematical analyses and transmission efficiency of a preloaded ball screw operating at high rotational speeds, Mechanism and Machine Theory, 46 (2011) 880-898.
22. Oh, K.-J., Khim, G., Park, C.-H., Chung, S.-C., Explicit modeling and investigation of friction forces in linear motion ball guides, Tribology International, 129 (2019) 16-28.

Figures and Tables:

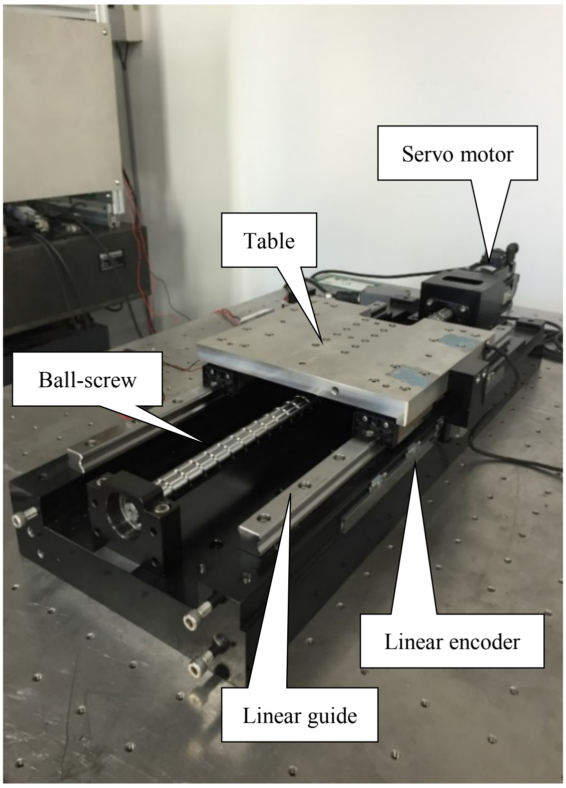

Figure 1 Feed drive mechanism

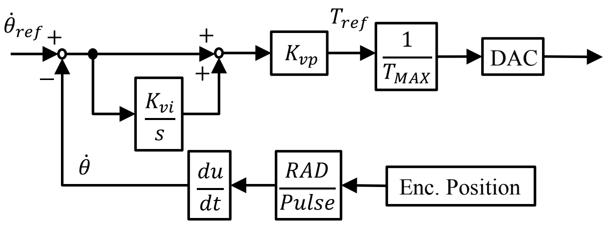

Figure 2 Block diagram of the control system

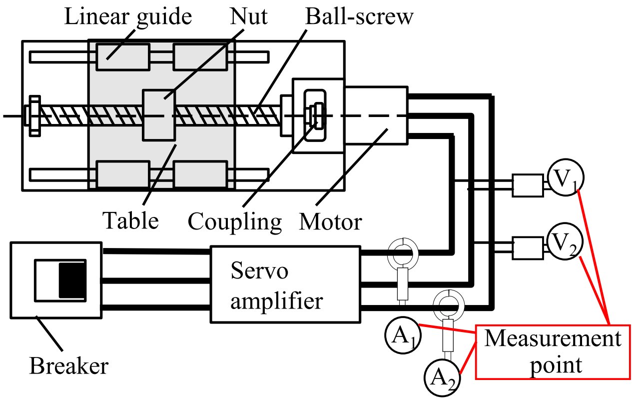

Figure 3 Electric power measurement apparatus

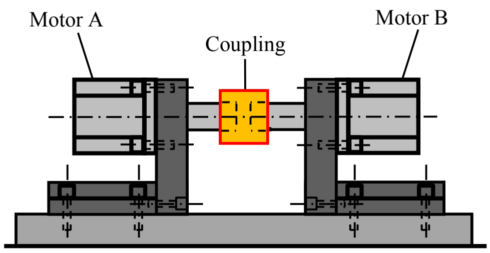

Figure 4 Experimental apparatus to evaluate the motor efficiency

Table 1 Specifications of motor and ball-screw

(a) Servo motor

Rated velocity	1500 rev/min
Rated torque	2.86 Nm
Rated power	450 W

(b) Ball-screws

Type	Lead [mm]	Nut (preload type)	Rotational torque of nut [Nm]
Ball-screw A (high preload)	20	Single (Oversize ball)	0.311
Ball-screw B (low preload)	10	Single (Oversize ball)	0.046
Ball-screw C (low preload)	5	Single (Oversize ball)	0.060
Ball-screw D (high preload)	5	Double (offset)	0.134

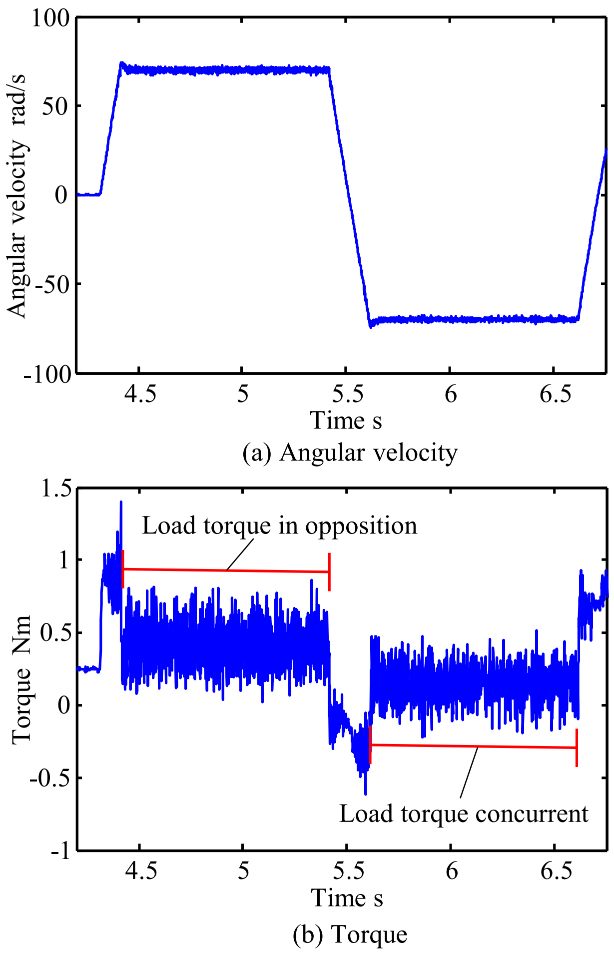

Figure 5 Example of measured angular velocity and motor torque during motion

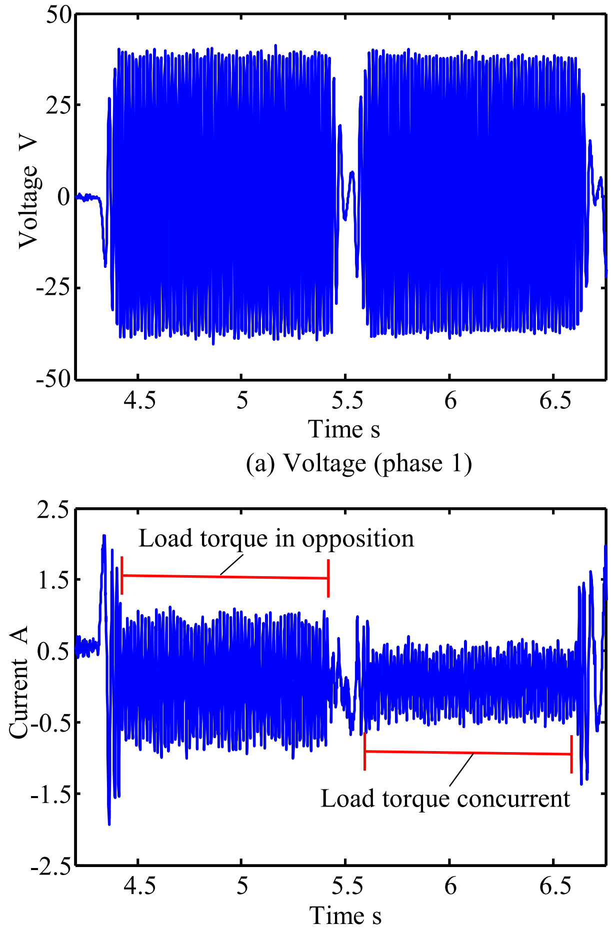

(a) Voltage (phase 1)

(b) Current (phase 1)

Figure 6 Example of measured voltage and current during motion

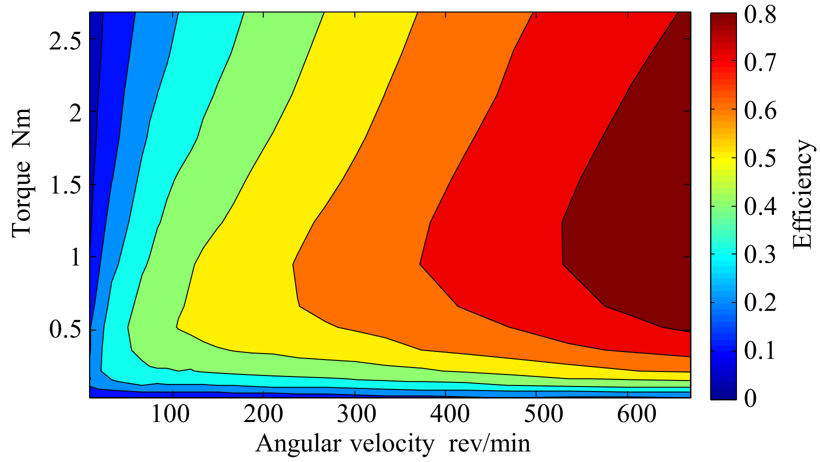

Figure 7 Measured efficiency map of the motor

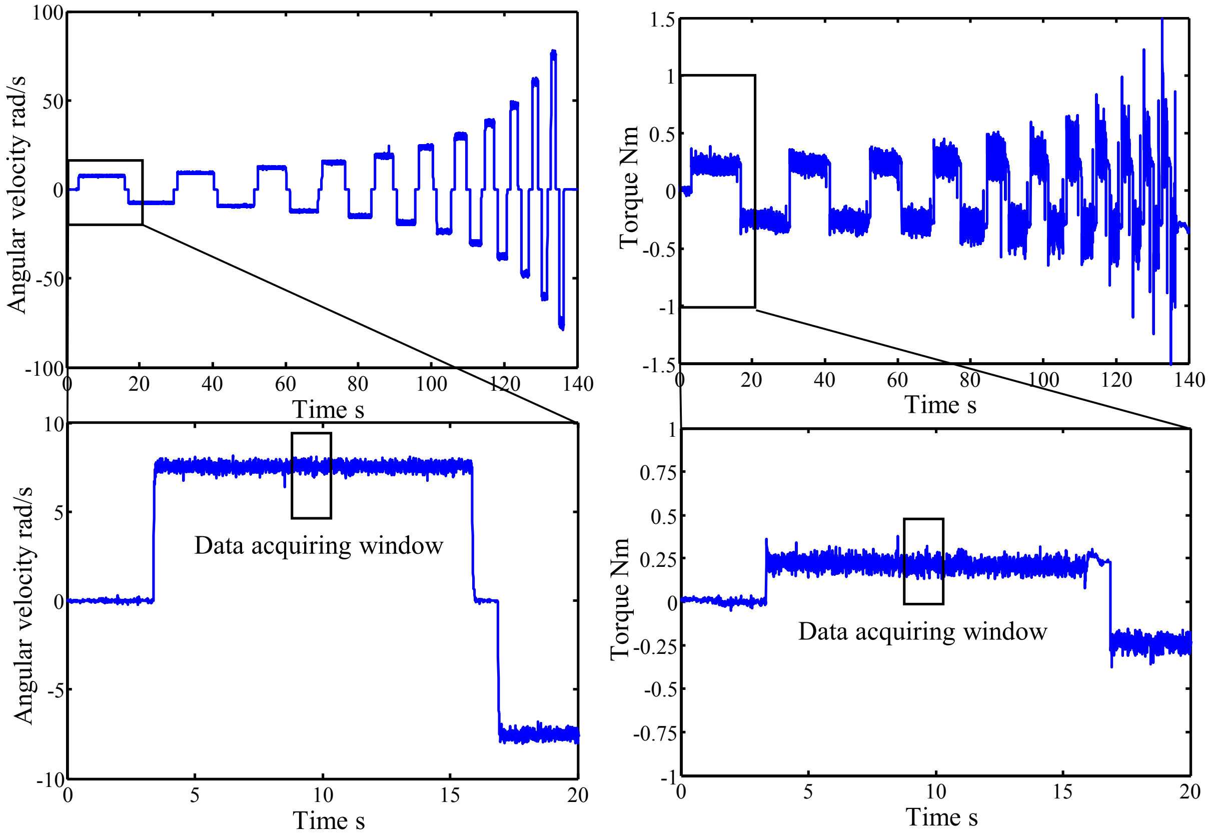

(a) Angular velocity
(b) Torque

Figure 8 Example of measured angular velocity and motor torque for the test with various velocities

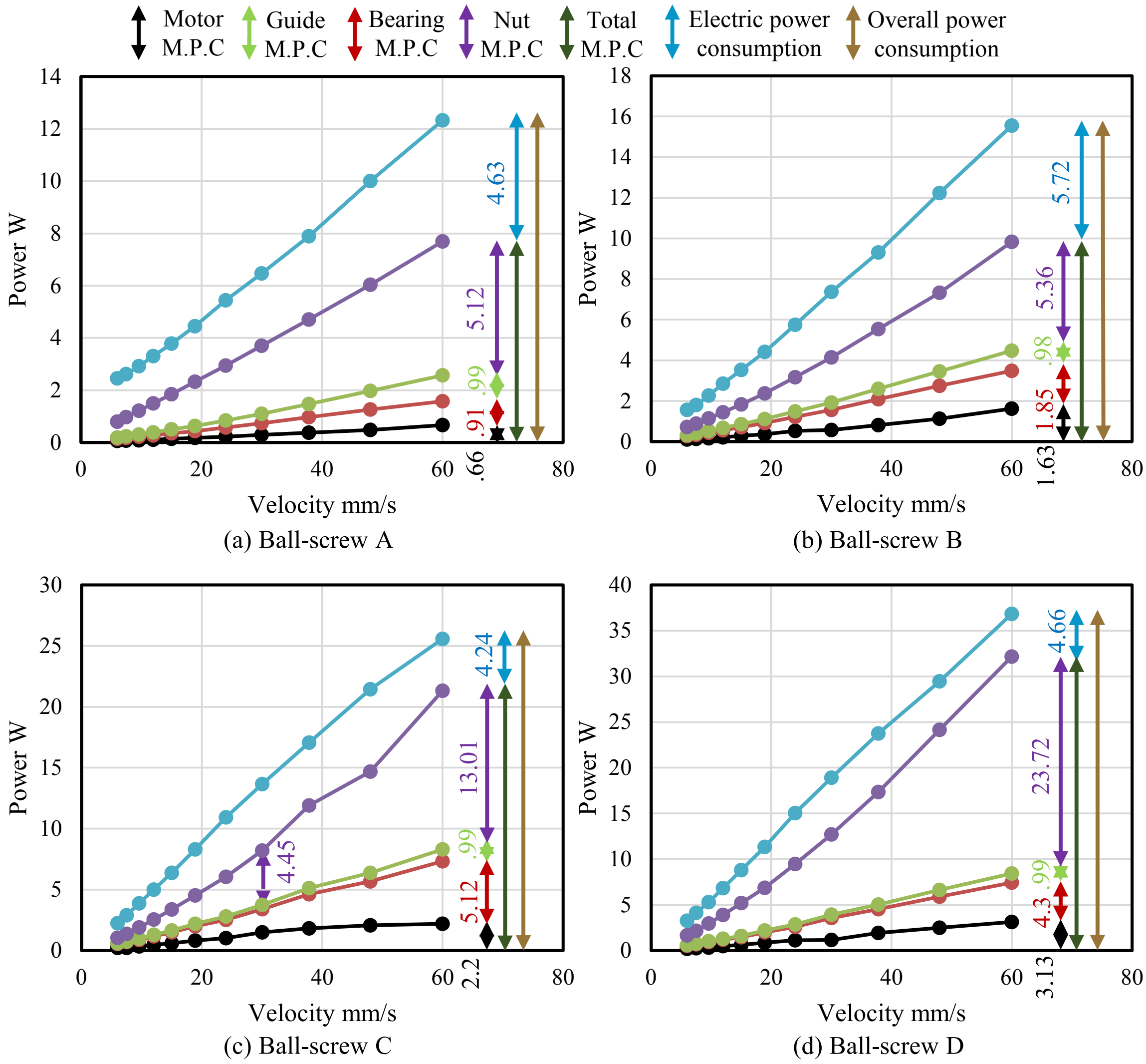

Figure 9 Comparison of the evaluated power consumption of each component

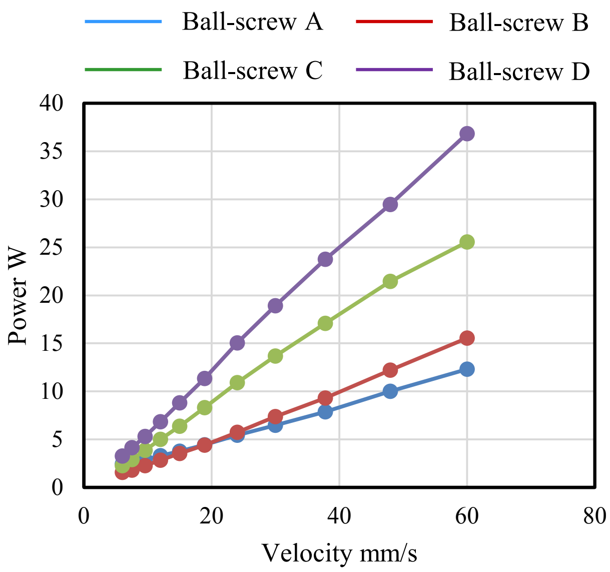

Figure 10 Comparison of the overall power consumption of each ball-screw

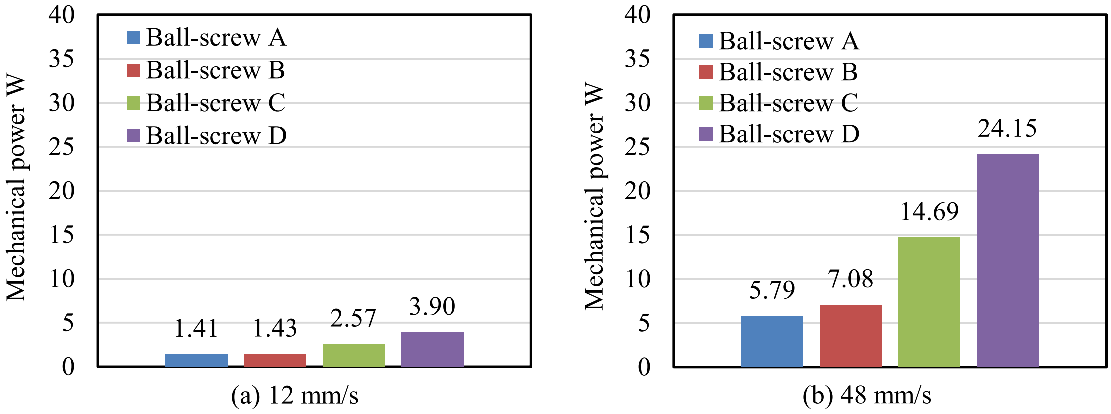

Figure 11 Comparison of mechanical power consumptions with different velocities

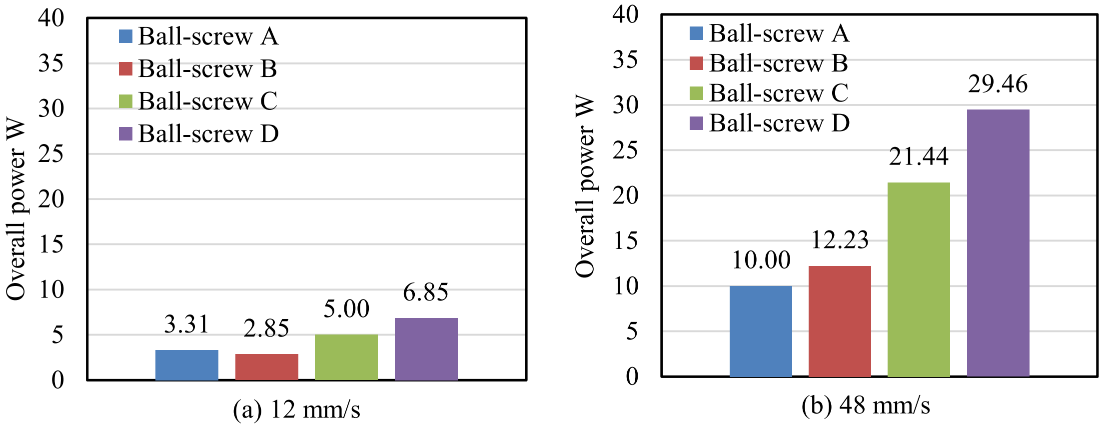

Figure 12 Comparison of overall power consumptions with different velocities

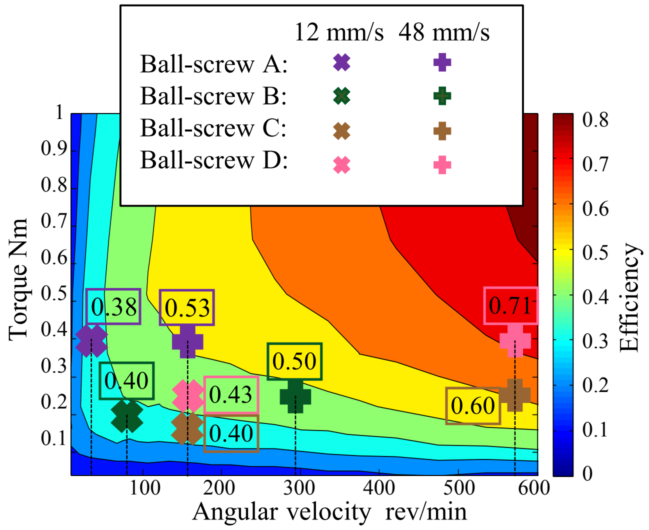

Figure 13 Comparison of the working condition of each ball-screw in the motor efficiency map

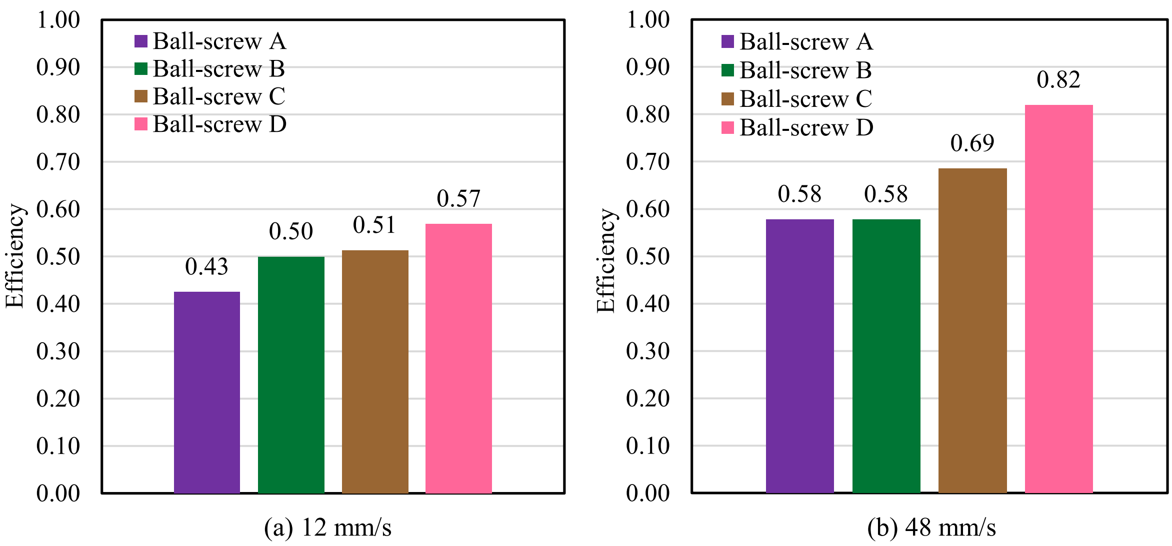

Figure 14 Comparison of motor efficiency for each condition